DMD Fast Forward. Published on August 21, 2015 as DOI: 10.1124/dmd.115.065623
This article has not been copyedited and formatted. The final version may differ from this version.

DMD #65623

**Title Page**

# P450-Based Drug-Drug Interactions of Amiodarone and its Metabolites: Diversity of Inhibitory Mechanisms.

*Matthew G. McDonald, Nicholas T. Au and Allan E. Rettie*

Department of Medicinal Chemistry, University of Washington, Seattle, WA: MGM, AER

Gilead Sciences Inc., Foster City, CA: NTA

DMD Fast Forward. Published on August 21, 2015 as DOI: 10.1124/dmd.115.065623
This article has not been copyedited and formatted. The final version may differ from this version.



**Running Title Page**

Running Title: Inhibitory metabolites in amiodarone drug-drug interactions

Corresponding author: Allan E. Rettie, Department of Medicinal Chemistry, University of Washington, Box 357610, Seattle, WA, 98195, USA; tele: (206)685-0615; fax: (206)685-3252; email: rettie@u.washington.edu

Text pages: 34

Tables: 2

Figures: 7

References: 42

Abstract: 249 words (250 limit)

Introduction: 593 words (750 limit)

Discussion: 1,411 words (1500 limit)

Abbreviations: AMIO, amiodarone; AUC, area under the time *vs* plasma drug concentration curve; CL, clearance; CYP, cytochrome P450 protein; DAA, deaminated-amiodarone; DDEA, N,N-didesethylamiodarone; DDI, drug-drug interaction; $ESI^+$-MS/MS, positive ion electrospray tandem mass spectrometry; HLM, human liver microsomes; MDEA, N-monodesethylamiodarone; MI complex, metabolitic intermediate complex; MRM, multiple reaction monitoring; ODAA, O-desalkylamiodarone; OH-MDEA, 3'-hydroxy-N-monodesethylamiodarone; PBPK, physiologically based pharmacokinetic modeling; TDI, time-dependent inhibition

## Abstract

$IC_{50}$ shift and time dependent inhibition (TDI) experiments were carried out to measure the ability of amiodarone (AMIO) and its circulating human metabolites to reversibly and irreversibly inhibit CYP1A2, CYP2C9, CYP2D6 and CYP3A4 activities in human liver microsomes. $[I]_u/K_{i,u}$ values were calculated and used to predict in vivo AMIO drug-drug interactions (DDIs) for pharmaceuticals metabolized by these four enzymes. Based on these values, the minor metabolite di-desethylamiodarone (DDEA) is predicted to be the major cause of DDIs with xenobiotics primarily metabolized by CYP1A2, CYP2C9 or CYP3A4, while AMIO and its mono-desethyl derivative (MDEA) are the most likely cause of interactions involving inhibition of CYP2D6 metabolism. AMIO drug interactions predicted from the reversible inhibition of the four P450 activities were found to be in good agreement with the magnitude of reported clinical DDIs with lidocaine, warfarin, metoprolol and simvastatin. TDI experiments showed DDEA to be a potent inactivator of CYP1A2 ($K_I$ = 0.46 μM, $k_{inact}$ = 0.030 $min^{-1}$), while MDEA was a moderate inactivator of both CYP2D6 ($K_I$ = 2.7 μM, $k_{inact}$ = 0.018 $min^{-1}$) and CYP3A4 ($K_I$ = 2.6 μM, $k_{inact}$ = 0.016 $min^{-1}$). For DDEA and MDEA, mechanism-based inactivation appears to occur through formation of a metabolic intermediate (MI) complex. Additional metabolic studies strongly suggest that CYP3A4 is the primary enzyme involved in the metabolism of AMIO to both MDEA and DDEA. In summary, these studies demonstrate both the diversity of inhibitory mechanisms with AMIO and the need to consider metabolites as the 'culprit' in inhibitory P450-based DDIs.

## Introduction

Amiodarone (AMIO) is a class III anti-arrhythmic agent, used widely to counter serious superventricular and ventricular tachyarrhythmias, and the most commonly used drug for treatment of patients with atrial fibrillation (Mason, 1987; Doyle and Ho, 2009). Although AMIO is an effective drug, its use has been complicated by safety issues, which are highlighted by several clinical reports linking pulmonary (Marchlinski et al., 1982; Heger et al., 1983), thyroidal (Dickstein et al., 1984), ocular (Castells et al., 2002) and/or liver (Rigas et al., 1986) toxicity to AMIO therapy. AMIO is also known to interact with a large variety of therapeutic agents, and many of these drug-drug interactions (DDIs) result from inhibition of cytochrome P450 (CYP) mediated metabolism, which raises systemic exposure of the 'victim' drug (Yamreudeewong et al., 2003).

Four specific P450 enzymes are implicated in the majority of these metabolism-dependent in vivo DDIs: CYP1A2 (lidocaine, theophylline), CYP2C9 (S-warfarin), CYP2D6 (metoprolol, flecainide) and CYP3A4 (cyclosporine A, simvastatin) (Soto et al., 1990; Nicolau et al., 1992; Chitwood et al., 1993; Funck-Brentano et al., 1994; Ha et al., 1996; Trujillo and Nolan, 2000; Orlando et al., 2004; Werner et al., 2004; Becquemont et al., 2007; Thi et al., 2009). AMIO, itself, appears to be a fairly weak in vitro inhibitor of these enzymes (Kobayashi et al., 1998; Ohyama et al., 2000), which raises the possibility that inhibitory metabolites play a more direct role than the parent drug. In fact, a recent literature review identified AMIO as one of only 5 out of 137 total pharmaceuticals to cause a metabolism-dependent clinical DDI judged to be due entirely to an inhibitory metabolite(s), with little to no contribution of the parent drug (Yu et al., 2015).

Therefore, a more complete analysis of AMIO-P450 inhibition should provide a useful case study for helping determine which future drugs are more at risk of a metabolism-dependent DDI caused by inhibitory metabolites.

Several circulating AMIO metabolites (Figure 1) have been identified (Ha et al., 2005) and these were investigated previously in our laboratory for their ability to contribute to the CYP2C9-mediated AMIO-warfarin DDI. Using $[I]_u/K_{i,u}$ ratios (i.e. unbound plasma concentration of the inhibitory metabolite, $[I]_u$, divided by the equilibrium constant for inhibition of warfarin 7-hydroxylation in human liver microsomes (HLM), normalized to the amount of free inhibitor available in those microsomes, ($K_{i,u}$)) we predicted the minor AMIO metabolite, N,N-didesethylamiodarone (DDEA) to be the 'culprit' most likely to induce the hypocoagulation effect seen when AMIO is co-administered with warfarin, (McDonald et al., 2012). Of course, $[I]_u/K_{i,u}$ ratios are most useful in predicting the inhibitor efficiency of purely reversible inhibitors, and there is conflicting evidence in the literature as to whether or not AMIO and/or its primary metabolite, N-monodesethylamiodarone (MDEA) can act as irreversible inhibitors of various P450 isozymes, including CYP2C9 (Ohyama et al., 2000; Obach et al., 2007; Berry and Zhao, 2008; Mori et al., 2009; Sekiguchi et al., 2009).

Therefore, the aim of this study was to predict, from in vitro studies, whether one or more of the circulating metabolites of AMIO might contribute to the CYP1A2, CYP2C9, CYP2D6 and CYP3A4-dependent DDIs that are observed in vivo with AMIO, through either reversible or metabolism-dependent inhibition. To this end, we used $IC_{50}$ shift and time-dependent inhibition (TDI) experiments to measure the inhibitory potential of AMIO and its circulating metabolites against diagnostic marker activities for each

P450 enzyme in HLM. We also identified the specific P450 enzyme(s) involved in the formation of the major inhibitory metabolites of AMIO to assess whether P450 polymorphisms are a potential variable in an individual's susceptibility to DDIs involving AMIO.

## Materials and Methods

*Materials.*

Midazolam was obtained as a 1mg/mL methanolic solution from Cerilliant (Round Rock, Tx). Diclofenac Sodium Salt, 1'-hydroxymidazolam-$d_4$, dextrorphan-$d_3$, 4'-hydroxydiclofenac-$d_4$ and acetaminophen-$d_3$ were purchased from Toronto Research Chemicals, Inc. (TRC, North York, ON). Paroxetine hydrochloride and montelukast sodium were procured from AvaChem Scientific (San Antonio, Tx), while troleandomycin and dextromethorphan were purchased from Enzo Life Sciences (Farmingdale, NY) and LKT Laboratories, Inc. (St. Paul, MN), respectively. Solvents were purchased from J.T. Baker, Inc. (Phillipsburg, N.J.) or Fischer Scientific (Springfield, N.J.). Unlabeled and deuterium-labeled AMIO metabolites were synthesized according to literature procedures (Wendt et al., 2002; Lucas et al., 2006; Waldhauser et al., 2006) or as previously described (McDonald et al., 2012). Pooled human plasma from healthy individuals, containing sodium citrate as an anticoagulant, was obtained from Innovative Research (Novi, MI). Cytochrome P450 Supersomes™ and Bactosomes™, expressed from cDNA using baculovirus infected insect cells, were, respectively, obtained from BD Biosciences (San Jose, CA) and XenoTech, LLC (Lenexa, KS). The P450s were all co-expressed with P450 oxidoreductase, as well as, in most cases, cytochrome $b_5$ (CYPs 1A1, 1A2, 1B1, 2C18, 2D6 and 4A11 were expressed without $b_5$). A set of pooled HLM was prepared from eight randomly selected human liver (HL) samples (HL 150, HL 151, HL 152, HL 154, HL 160, HL 166 HL 167 and HL 169) from the Human Liver Bank that is maintained within the Department of Medicinal

Chemistry at the University of Washington using established protocols (Sadeque et al., 1992). Additional HLM pools were prepared from human liver samples HL 119 (CYP2D6*4*4), HL 167 (*41*41) and HL 168 (*4*4) (CYP2D6 poor metabolizers) and HL 132, HL 143 and HL 150 (CYP2D6*1*1 extensive metabolizers), respectively. All other chemicals used in this study were purchased from Sigma-Aldrich Chemical Co. (St. Louis, MO).

*AMIO/MDEA Metabolic Assays*

AMIO or MDEA (5 μM) was incubated with either HLM (at final concentrations ranging from 0.25 to 1.0 mg/mL microsomal protein) or P450 Supersomes$^{TM}$ (20 pmol) in 50 mM potassium phosphate buffer, pH 7.4, containing 4% bovine serum albumin, in a 250 μL volume with 1% v/v of methanol. After 2 minutes pre-incubation at 37 $^{o}$C/70 rpm, the reactions were initiated with NADPH (1mM final concentration), and then incubated for a further 30 min at 37$^{o}$C/70 rpm prior to quenching with 25 μL of a 15% aqueous $ZnSO_4$ solution. MDEA-d4 and DDEA-d4 were added as internal standards. The quenched reactions were extracted with ethyl acetate and the organic phase was collected and evaporated under nitrogen gas. The residue was then re-dissolved in 50 μL methanol for LCMS analysis.

*AMIO/MDEA Chemical Inhibition Assay*

AMIO or MDEA (5 μM) incubations with HLM as the enzyme source (1 mg/mL) were carried out under the conditions listed above, but with the further addition of a specific chemical P450 inhibitor (i.e. α-naphthoflavone (1 μM final concentration),

furafylline (10 μM), montelukast (1 μM), sulfaphenazole (10 μM), N-benzylnirvanol (1 μM), quinidine (1 μM), ketoconazole (3 μM), or troleandomycin (50 μM)) added to the pre-incubation mix. Incubations were carried out in triplicate for each inhibitor as well as for a no inhibitor positive control. Final reaction volumes contained 1% methanol.

*DDEA Ki Studies*

Incubation mixtures contained 0.25 mg/mL microsomal protein from the HLM pool and 0.5% v/v of a 200x concentrated methanolic DDEA stock solution (5 different stocks, generating final concentrations between 0 and 2 μM) with either midazolam (at 0.5, 2 or 8 μM final concentration), diclofenac (at 1, 4 or 16 μM) or phenacetin (at 10, 40 or 160 μM) added as substrate (from 100x concentrated 50% aqueous methanolic stock solutions) in 100 mM potassium phosphate buffer, pH 7.4 (KPi). After a 2 minute pre-incubation at 37$^{o}$C/70 rpm in a water bath, the reactions were initiated with NADPH (1 mM final concentration, 250 μL final reaction volume) and were incubated for an additional 30 minutes. Reactions were quenched by addition of an equal volume of acetonitrile (containing either 50 nM of 1'-hydroxymidazolam-$d_4$, 100 nM of 4'-hydroxydiclofenac-$d_4$ or 5 μM of acetaminophen-$d_3$ as internal standard), centrifuged to remove protein and the supernatants analyzed by LCMS. All incubations were carried out in triplicate.

*$IC_{50}$ Shift Experiments*

Cocktail assay: In a 96-well plate, wells 1-24 and 25-48 both contained inhibitor, (added from 8 different 200x concentrated methanolic stock solutions – done in triplicate

replications) and pooled HLM (final concentration = 0.25 mg/mL microsomal protein) in KPi buffer. After 2 minutes preincubation at 37°C, 2.5 µL of NADPH stock (wells 1-24, final conc = 1 mM) or buffer without NADPH (wells 25-48) were added; final incubation volume = 250 µL. The plate was incubated at 37°C for 30 minutes, then 196 µL was removed from each well and added to a second plate containing 2 µL of a 100x concentrated substrate cocktail stock (in 50% aqueous methanol, final incubation concentrations = 4 µM diclofenac, 4 µM dextromethorphan and 2 µM midazolam) per well, plus 2 µL of either buffer only (wells 1-24) or buffer with NADPH (1 mM final concentration, wells 25-48). This plate was incubated for 5 minutes at 37°C prior to quenching with equal volumes of acetonitrile containing 50 nM 1'-hydroxymidazolam-$d_4$, 50 nM dextrorphan-$d_3$ and 100 nM 4'-hydroxydiclofenac-$d_4$ as internal standards.

The phenacetin O-dealkylation $IC_{50}$ shift assay was carried out using identical methodology, however a stock solution of 4 mM phenacetin (giving a 40 µM final incubation concentration) was used in place of the substrate cocktail, while the acetonitrile quench solution was similarly replaced with a 5 µM solution of acetaminophen-$d_3$ as internal standard. All $IC_{50}$ shift assays were performed at least twice and data are presented as mean values with standard error measurements.

In some experiments, with MDEA as inhibitor, glutathione or N-acetylcysteine (10 mM each) were added as trapping agents for reactive intermediates.

*Time Dependent Inhibition (TDI) Experiments*

Cocktail assay: Incubations were carried out in 1.2 mL library tubes for each of six inhibition concentrations (added from 200x concentrated methanolic stock), in

duplicate replications. Each incubation contained 0.25 mg/mL pooled HLM in KPi buffer. The tubes were pre-incubated at 37 $^{o}$C/70 rpm for two minutes in a water bath prior to initiation with NADPH (1 mM in 1.1 mL final volume). At times 0, 5, 10, 15 and 20 minutes, 198 µL aliquots were removed from each library tube and added to 2 µL of a 100x concentrated substrate cocktail stock solution (in 50% aqueous methanol) to give final concentrations of 40 µM diclofenac, 40 µM dextromethorphan and 20 µM midazolam. The substrate reactions were then incubated for 5 minutes at 37 $^{o}$C/70 rpm before quenching with an equal volume of acetonitrile standard solution (containing 50 nM 1'-hydroxymidazolam-$d_4$, 50 nM dextrorphan-$d_3$ and 100 nM 4'-hydroxydiclofenac-$d_4$).

Again, the phenacetin O-dealkylation TDI experiment was carried out using identical methodology, except that a stock solution of 20 mM phenacetin (200 µM final incubation concentration) was used in place of the substrate cocktail, while the acetonitrile quench solution was replaced with a 5µM solution of acetaminophen-$d_3$ as internal standard.

*LCMS Analysis*

LCMS analyses were conducted on a Micromass Quattro Premier XE Tandem Quadrupole Mass Spectrometer (Micromass Ltd., Manchester, U.K.) coupled to an ACQUITY Ultra Performance LC™ (UPLC™) System with integral autoinjector (Waters Corp., Milford, MA). The Premier XE was operated in ESI$^{+}$-MS/MS (MRM) mode at a source temperature of 120$^{o}$C and a desolvation temperature of 350$^{o}$C. The following mass transitions were monitored in separate ion channels for the substrate

cocktail assay: *m/z* 258 > 157 (dextrorphan-$d_0$), *m/z* 261 > 157 (dextrorphan-$d_3$), *m/z* 312 > 230 (4'-hydroxydiclofenac-$d_0$), *m/z* 316 > 234 (4'-hydroxydiclofenac-$d_4$), *m/z* 342 > 324 (1'-hydroxymidazolam-$d_0$) and *m/z* 346 > 328 (1'-hydroxymidazolam-$d_4$) at cone voltages of 25, 23 and 30V and collision energies of 35, 33 and 35 eV for dextrorphan, 4'-hydroxydiclofenac and 1'-hydroxymidazolam, respectively. For the phenacetin O-dealkylation assay, mass transitions of *m/z* 152 > 110 (acetaminophen-$d_0$) and *m/z* 155 > 110 (acetaminophen-$d_3$) were monitored at a cone voltage of 25 V and a collision energy of 17 eV. Mass spectral data analyses were carried out on Windows XP-based Micromass MassLynxNT®, v 4.1, software.

Metabolic products from the substrate cocktail incubations were separated on an Acquity BEH $C_8$, 1.7 μ, 2.1 x 50 mm, UPLC column (Waters, Corp) using a binary solvent gradient where solvent A = 0.05% aqueous formic acid and solvent B = methanol, with a constant flow rate of 0.35 mL/min. From 0 to 1 minute, solvent was set at 5% B and was then increased linearly to 95% B from 1 to 2.5 minutes, where it was maintained for 0.5 minutes and then re-equilibrated to 5% B over 0.2 minutes. The same Acquity $C_8$ UPLC column was used to analyze products from the phenacetin O-dealkylation assay, but using a binary solvent system where solvent A = 10 mM ammonium acetate (pH 4.6) and solvent B = methanol. From 0 to 0.75 minutes, the solvent was delivered isocratically at 5% B and was then increased linearly to 95% B over an additional 1.25 minutes, where it was maintained for 1 minute and then re-equilibrated to 5% B over 0.2 minutes. The flow rate was again maintained at 0.35 mL/min.

MDEA and DDEA were analyzed quantitatively as previously described (McDonald et al., 2012).

*P450 Binding Studies*

Difference binding spectra were recorded on an Olis modernized Aminco DW-2 spectrophotometer (Olis, Bogart, GA). Sample and reference cuvettes contained 100 to 200 nM P450 Supersomes™ in 100 mM KPi buffer at pH 7.4, and a baseline scan was performed at 25°C. Blank solvent or aliquots from a concentrated stock solution, respectively, were added to the reference and sample cuvettes to give final inhibitor concentrations between 5 and 40 μM. To determine the mode of inhibitor binding, absorbance was recorded at 25°C over a spectroscopic range from 350 to 500 nm and the resultant spectra were corrected for baseline drift.

*MI-Complex Formation*

MI complex formation was also monitored on an Olis modernized Aminco DW-2 specrtrophotometer (Olis). Sample and reference cuvettes contained either 1 mg/mL pooled HLM, 110 nM P450 Supersomes™ or 400 nM P450 Bactosomes™, along with 5-40 μM inhibitor, in 100 mM KPi buffer at pH 7.4. After 3 minutes pre-incubation at 37°C, blank KPi buffer and NADPH in KPi buffer were added to the reference and sample cuvettes, respectively (to 1 mM final NADPH concentration). The cuvettes were then scanned repetitively over an optical range from 495 to 430 nm in 5 nm increments (0.1 min/scan), for 25 minutes, while maintaining temperature at 37°C.

*Data Analysis*

GraphPad Prism v 5.0 software was used in the graphing/analyses of results from all metabolic assays and inhibitory enzyme kinetic experiments.

## Results

### *$IC_{50}$ Shift Experiments*

AMIO and its circulating metabolites were tested for their ability to inhibit four specific P450 metabolic activities in pooled HLM. Phenacetin O-dealkylation was used to probe CYP1A2 activity, while diclofenac 4'-hydroxylation, dextromethorphan O-dealkylation and midazolam 1'-hydroxylation were used as specific activity probes for CYP2C9, CYP2D6 and CYP3A4, respectively. Inhibitory potency against CYP2C9, CYP2D6 and CYP3A4 activities was measured in HLM using a substrate cocktail assay, as diclofenac, dextromethorphan and midazolam showed no P450 cross inhibition at their relative $K_m$ substrate concentrations (data not shown). $IC_{50}$ shift experiments were all run at the reported $K_m$ values for the substrates, i.e. 40 μM for phenacetin, 4 μM for diclofenac, 4 μM for dextromethorphan and 2 μM for midazolam (Kobayashi et al., 1998; Yuan et al., 2002; Berry and Zhao, 2008). Using a conservative approach, we estimated $K_i$ values as ½ of the $IC_{50}$ values determined for each inhibitor in the absence of NADPH pre-incubation in their respective $IC_{50}$ shift experiments (i.e. reversible inhibition was assumed to be competitive). $[I]_u/K_{i,u}$ ratios were calculated for AMIO and its metabolites using previously determined plasma concentrations along with fraction unbound values for each of these compounds that were previously measured in both plasma and microsomes (McDonald et al., 2012). The $IC_{50}$ values for the reversible inhibition of CYP1A2, CYP2C9, CYP2D6 and CYP3A4 activities in HLM, by the various AMIO metabolites, are shown in Table 1. Due to poor inhibitor solubility, $IC_{50}$ values above ~50-100 μM could not be measured reliably.

For a drug with multiple inhibitory metabolites, such as AMIO, the total change in clearance affected by the reversible inhibition of a specific P450 isozyme can be predicted according to Equation 1 (Templeton et al., 2008). Since the AMIO metabolites are all highly protein bound in plasma and/or HLM, the accuracy of the prediction should be greatly improved by substituting with $[I]_u/K_{i,u}$ ratios, as this corrects for the amount of freely available inhibitor in both plasma and in HLM. Summing together the $[I]_u/K_{i,u}$ ratios shown in Table 1 allows us to predict clinical drug-drug interactions arising from the inhibition of CYP1A2, CYP2C9, CYP2D6 and CYP3A4 metabolism by AMIO (Table 2).

$$DDI \equiv CL/CL_{inhibited} = AUC_i/AUC = 1 + \sum [I]/K_i \qquad \text{(Equation 1)}$$

Furafylline (FF), tienilic acid (TA), paroxetine (PAR) and troleandomycin (TAO) are specific mechanism-based inactivators of CYP1A2, CYP2C9, CYP2D6 and CYP3A4, respectively, and so were used as positive controls for these $IC_{50}$ shift experiments (Berry and Zhao, 2008; Parkinson et al., 2011). As expected, these compounds all showed significant TDI, exhibiting $IC_{50}$ shifts (i.e. the ratios of the inhibitor $IC_{50}$ values determined without *versus* with a 30 minute inhibitor/NADPH pre-incubation step) of between 9.4 (PAR/CYP2D6) and 40 (TAO/CYP3A4). By contrast, the largest $IC_{50}$ shift we observed for parent drug or AMIO metabolite was 3.1, determined for the inhibition of CYP2D6 activity by MDEA, or roughly twice the generally accepted significance threshold for a TDI (Parkinson et al., 2011). Inclusion of glutathione and N-

acetylcysteine in microsomal incubations modestly reduced the $IC_{50}$ shift ratios for CYP2D6, CYP3A4 and CYP2C9 activities to between 1.5 and 2.1 (data not shown).

*DDEA Ki Experiments*

Since, to our knowledge, the importance of DDEA as an inhibitory metabolite in AMIO therapy has not been previously addressed, we more fully explored its mechanism of inhibition against the P450s for which it exhibits the greatest inhibitor potency. Also, due to the relatively low $IC_{50}$ values obtained for the inhibition of CYP2C9 and CYP3A4 activities in HLM, and the observation that DDEA is 99% bound in HLM under the experimental conditions (McDonald et al., 2012), we were concerned that a low free inhibitor:enzyme ratio could potentially mask tighter binding of the inhibitor to these enzymes.

Therefore, full kinetic analyses to determine $K_i$ values was performed separately for the inhibition by DDEA of phenacetin O-dealkylation, diclofenac 4'-hydroxylation and midazolam 1'-hydroxylation activities in HLM. The $K_i$ values obtained were 723 ± 81 nM for the inhibition of CYP1A2, 308 ± 20 nM for the inhibition of CYP2C9 and 1.15 ± 0.38 μM for the inhibition of CYP3A4. DDEA appears to inhibit all three enzymes competitively, although there may be a mixed component to the inhibition of CYP1A2 (Figure 2A-C).

*Time Dependent Inhibition Experiments*

AMIO, MDEA and DDEA were selected for further testing in TDI experiments with CYPs 1A2, 2C9, 2D6 and 3A4 using HLM as the enzyme source. As in the $IC_{50}$ shift experiments, CYP1A2 inhibition was studied separately, while a substrate cocktail assay was used to test inhibition of the latter three drug metabolizing enzymes. Substrate concentrations were used at 10x their reported $K_m$ values (5x $K_m$ for phenacetin). Diclofenac, dextromethorphan and midazolam again showed minimal P450 cross inhibition even at these elevated concentrations.

AMIO was found not to be inhibitory towards CYP1A2, but both MDEA and DDEA inhibited phenacetin O-dealkylation activity in HLM in a time-dependent manner. Solubility issues precluded an accurate measurement of the inactivation parameters for MDEA ($K_I$ > 40 μM), while DDEA proved to be a potent inactivator of CYP1A2 with a $K_I$ = 0.46 μM and a $k_{inact}$ = 0.030 $min^{-1}$ (Figure 3A). DDEA competitively inhibited CYP2C9, CYP2D6 and CYP3A4 activities with no TDI component, while AMIO and MDEA were poor inactivators of CYP2C9-mediated diclofenac 4'-hydroxylation in HLM ($K_I$'s > 40 μM). AMIO also appeared to be a poor inactivator of CYP3A4, with an intermediate $K_I$ of 4.7 μM, but a low $k_{inact}$ value of less than 0.01 $min^{-1}$. In contrast, MDEA was a more potent time-dependent inhibitor of both CYP2D6 and CYP3A4 activity, exhibiting almost identical $K_I$ (2.7 μM and 2.6 μM) and $k_{inact}$ values (0.018 $min^{-1}$ and 0.016 $min^{-1}$) for both enzymes (Figure 3B and 3C).

*P450 Binding Studies*

Type I binding occurs when a P450 substrate or inhibitor displaces the water molecule directly coordinated to the distal side of the heme iron in the enzyme active site,

thus changing the oxidation state of the iron from 'low spin' to 'high spin', and produces a difference spectrum with a Soret maximum at 385-390 nm and a trough at around 420 nm. In Type II binding, the inhibitor (usually a primary amine) again displaces the water molecule from the heme while also coordinating directly to the iron atom, leaving the iron in a (perturbed) 'low spin' state. As a result of this energetically favorable heme coordination, Type II compounds are generally believed to bind more tightly to P450 enzymes than analogous Type I binders, resulting in stronger inhibition profiles. They produce a difference spectrum with a Soret maximum at 420-435 nm and a trough at 390-405 nm (Jefcoate, 1978).

As expected, the primary amine, DDEA, produced a difference spectrum consistent with Type II binding with CYP1A2, CYP2C9 and CYP2D6 (Figure 4). By contrast, the secondary amine, MDEA, bound weakly to CYP2D6 in Type I fashion. We were unable to generate binding spectra for either AMIO or MDEA with CYP3A4 Supersomes™.

*MI Complex Formation*

Oxidative metabolism of primary and secondary amines by P450 enzymes can sometimes lead to TDI of those P450s *via* the formation of metabolic intermediate (MI) complexes. These complexes are believed to arise through the irreversible coordination of a nitroso-amine metabolite to the heme iron, within the P450 active site, and they exhibit a signature Soret absorbance maximum at around 455 nm by difference spectroscopy (Hanson et al., 2010).

Among the AMIO metabolites tested, formation of an MI complex was observed only upon incubation of MDEA with CYP2D6 and CYP3A4, and of DDEA with CYP1A2. The maximum absorbance ($\lambda_{max}$) values for the MDEA MI complexes were at 458 (CYP2D6) and 455 nm (CYP3A4), while $\lambda_{max}$ for the DDEA-CYP1A2 MI complex was measured at 454 nm (Figure 5). BD Gentest Supersomes™ (at 110 nM P450 concentration) were used in the experiments involving CYP2C9, CYP2D6 and CYP3A4. We were unable to perform similar experiments with CYP1A2 Supersomes™ due to presumed enzyme stability issues, likely explained by the observation that pre-incubation of the Supersomes with NADPH resulted in rapid enzyme inactivation even in the absence of inhibitor (data not shown). Therefore, the MI complex experiments with CYP1A2 were performed with XenoTech Bactosomes™ at a P450 concentration of 400 nM. Using an extinction coefficient of 65 $cm^{-1}mM^{-1}$, which has been previously reported for the 455 to 490 absorbance difference (Liu and Franklin, 1985), we could calculate the percentage of MI complex formed in relation to the total initial enzyme concentration in the reaction mixture. The secondary amine, MDEA, exhibited a higher percentage of MI complex with CYP2D6 (9.1%) and, especially, with CYP3A4 (45%) than did the primary amine, DDEA, with CYP1A2 (5.8%).

*Amiodarone Metabolism by Cytochrome P450 Enzymes*

Next, we screened for AMIO N-deethylase activity across a range of recombinant human P450 Supersomes™ (Figure 6A). Although CYP1A1 showed the greatest overall metabolic activity, at 810 ± 77 pmol MDEA formed/min/nmol enzyme, CYP3A4 exhibited the highest activity among the major drug-metabolizing enzymes in the liver

(520 ± 99 pmol/min/nmol). CYPs 1A2, 2C8, 2C19, 2D6, 2J2 and 3A5 also catalyzed low to moderate AMIO N-deethylase activity. When AMIO metabolism was studied in HLM, the specific CYP3A4 chemical inhibitors, troleandomycin and ketoconazole both reduced MDEA formation by roughly 90%, while furafylline (specific inhibitor of CYP1A2), montelukast (CYP2C8), sulfaphenazole (CYP2C9), N-benzylnirvanol (CYP2C19) and quinidine (CYP2D6) were all essentially non-inhibitory towards AMIO N-deethylation (Figure 6B).

We next screened for MDEA N-deethylase activity across a similar range of recombinant drug metabolizing P450 enzymes (Figure 7A). Interestingly, CYP2D6 Supersomes$^{TM}$ were found to be most active in producing DDEA, which was formed at a rate of 500 ± 20 pmol/min/nmol enzyme, while recombinant CYPs 1A1 and 3A4 were only ~20% as effective. However, when using specific chemical inhibitors against the HLM-catalyzed reaction, the CYP3A4 inhibitors, ketoconazole and troleandomycin, were again the most effective in reducing N-deethylation (by 94% and 87%, respectively), while quinidine inhibited DDEA formation by, at most, 10-20% (Figure 7B). To resolve this apparent discrepancy, we combined three HLM samples from CYP2D6 poor metabolizers and three HLM samples from CYP2D6 extensive metabolizers and compared the MDEA-deethylase activity of the CYP2D6 poor metabolizer pool (3.50 ± 0.20 pmol/min/nmol total P450) with that of the extensive metabolizer pool (3.91 ± 0.25 pmol/min/nmol P450). These data suggest strongly that CYP2D6 is not a major contributor to MDEA-deethylase activity in HLM, an activity that is instead dominated by CYP3A4.

**Discussion**

In the course of pre-clinical drug discovery in the pharmaceutical industry, $IC_{50}$ shift experiments are commonly used to screen out compounds that act as time dependent inhibitors of the major human liver P450s (Obach et al., 2007; Parkinson et al., 2011). If TDI of the enzyme is occurring, a 30 minute pre-incubation of a drug candidate in the presence of NADPH should result in increased inhibitory potency relative to a 30 minute incubation of the compound in the absence of cofactor (lowering the former $IC_{50}$ and thus shifting it to the left of the latter curve). Generally, a ratio of the non-shifted (preincubated minus NADPH) to shifted $IC_{50}$ (preincubated with NADPH) of greater than ~1.5 is used as an indicator of potential TDI (Parkinson et al., 2011).

Alternatively, $IC_{50}$ shift experiments can be used to predict the potential for a compound to cause an in vivo interaction due to the reversible inhibition of a specific drug metabolizing enzyme. If we assume that the mode of inhibition is competitive, then the reversible $IC_{50}$ component of the experiment, carried out at the $K_m$ for the substrate, should be equal to twice the value of the inhibitor $K_i$. Guidelines issued by the U.S. Food and Drug Administration for the prediction of an in vivo drug interaction from in vitro data are based upon $[I]/K_i$ ratios, i.e. the total plasma concentration of the drug candidate divided by its in vitro inhibition constant, usually measured in HLM (U.S._Food_and_Drug_Administration, 2006). If the $[I]/K_i$ ratio is below 0.1 then the likelihood that the compound will lead to an interaction with other drugs metabolized by the enzyme in question is considered to be remote. Compounds with a ratio between 0.1

and 1.0 or with a ratio > 1.0 are considered to be possible and likely contributors, respectively, to potential DDIs involving a given enzyme

The results from the $IC_{50}$ shift experiments, showing only the reversible inhibition of CYP1A2, CYP2C9, CYP2D6 and CYP3A4 metabolic activities by AMIO and its circulating metabolites, are given in Table 1. When presented in terms of $[I]_u/K_{i,u,}$ (i.e. correcting the $[I]/K_i$ ratios for plasma and microsomal protein binding) the data indicate that the Type II inhibitor DDEA is likely to be the major perpetrator in inhibitory DDIs that involve CYP1A2, CYP2C9 and CYP3A4. By contrast, it appears that AMIO and MDEA, but not DDEA, are likely to be the major contributors to DDIs involving CYP2D6. If we apply Equation 1 to the results listed in Table 1, we can predict the overall change in clearance (CL) due to concomitant AMIO therapy for drugs primarily metabolized by each of the four P450s examined here. Several in vivo DDIs caused by AMIO inhibition of CYP1A2, CYP2C9, CYP2D6 or CYP3A4-mediated metabolism have been previously quantified and show very good agreement with our in vitro data (Table 2).

We next considered the ability of AMIO and its metabolites to act as time-dependent inhibitors, but the $IC_{50}$ shift experiments provided scant evidence for possible TDI. The highest recorded $IC_{50}$ shift ratio, for MDEA-dependent inactivation of CYP2D6, was ~3, a value that was only slightly reduced by inclusion of reactive intermediate trapping agents. Nevertheless, AMIO, MDEA and DDEA were included in more detailed TDI experiments designed to provide a fuller kinetic characterization of their time-dependent inhibition. All three compounds inactivated one or more of the P450s studied, although only the two N-dealkylated metabolites showed more than weak

inactivation profiles for any of the enzymes; DDEA proving to be a potent time-dependent inhibitor of CYP1A2, and MDEA showing moderate inactivation of both CYP2D6 and CYP3A4 (Figure 3).

There are two major mechanisms by which a compound exhibits mechanism based inactivation of P450 enzymes: oxidative metabolism can lead to a reactive intermediate capable of alkylating either the protein or prosthetic heme group or, alternatively, if the inhibitor structure contains an amine functional group, N-oxidation can then lead to the formation of an irreversible metabolic intermediate (MI) complex between a nitroso group and the heme iron (Hanson et al., 2010; VandenBrink and Isoherranen, 2010). Although there are literature data that point to the ability of AMIO to form at least trace amounts of a reactive o-quinone metabolite in rat liver microsomes, feces and urine, the o-quinone was not detected as a circulating metabolite in plasma (Varkhede et al., 2014). Additionally, the inclusion of nucleophilic trapping agents in our human liver microsomal experiments did not substantially protect against modest enzyme inactivation induced by MDEA in $IC_{50}$ shift experiments. Therefore, while inactivation of certain recombinant P450 enzymes can be demonstrated by some AMIO metabolites in vitro, irreversible P450 inhibition in HLMs is a relatively minor event. While the observation of MI complex formation between MDEA and both CYP2D6 and CYP3A4,as well as between DDEA and CYP1A2 upon incubation with NADPH is interesting and novel, we should acknowledge that the overall accumulation of MI complex was low (5 - 45% of maximum, based on initial enzyme concentration) even with experimental inhibitor concentrations greatly exceeding those encountered under physiological conditions. Therefore, irreversible and quasi-irreversible P450 inhibition

DMD Fast Forward. Published on August 21, 2015 as DOI: 10.1124/dmd.115.065623
This article has not been copyedited and formatted. The final version may differ from this version.



are likely minor mechanisms contributing to inhibitory P450 DDIs that arise during AMIO treatment.

Interestingly, a recently published PBPK study utilized previously reported values for the reversible and time dependent inhibition parameters of AMIO and MDEA to predict potential DDIs involving CYP2C9, CYP2D6 and CYP3A4-mediated metabolism (Chen et al., 2015). Not surprisingly, since kinetic inhibition parameters can often differ considerably depending on the literature source, there are some significant differences in the $K_i$, $K_I$ and $k_{inact}$ values the authors use to generate their predictions compared to those reported here. However, it is of particular interest that, considering only AMIO and MDEA inhibition parameters, the model of Chen et al., (2015) appears to substantially under-predict the well known warfarin-AMIO DDI. This discrepancy is in line with our contention that the minor AMIO metabolite, DDEA, is the primary culprit in AMIO DDIs involving CYP2C9. The authors' PBPK model performs very well for predictions of AMIO DDIs involving CYP2D6 and CYP3A4 metabolism. Our own predictions for AMIO DDIs involving CYP2D6 and CYP3A4 also appear to be reasonable (Table 2), despite the fact that the parameters we use to arrive at our predictions differ from those used in the PBPK study. It is possible that our slight under-prediction of these DDIs could result from the lack of incorporation into our model of MDEA kinetic parameters for modest time-dependent inhibition of CYP2D6 and CYP3A4 metabolism.

Finally, because MDEA and DDEA both appear to be likely contributors to the in vivo drug interactions of AMIO, there exists the possibility that polymorphism within genes responsible for metabolite formation could lead to individual variation in the magnitude of these DDIs. Multiple metabolic approaches performed with AMIO or

MDEA using recombinant P450 enzymes, pooled HLM with specific chemical P450 inhibition probes, or with CYP2D6 genotyped HLM, all strongly suggest that CYP3A4 is primarily responsible for the production of both N-dealkylated metabolites. Since there is no evidence in the literature that any correlation exists between CYP3A4 polymorphism and in vivo DDIs, it is unlikely that differences in an individual's susceptibility to AMIO-induced drug interactions can be attributed to a pharmacogenetic effect on the rate of formation of MDEA or DDEA from AMIO, although it is still possible that genetic variation in P450s could lead to differences in MDEA or DDEA clearance.

In conclusion, this report implicates AMIO and two of its metabolites, MDEA and DDEA, as major contributors to in vivo drug interactions involving multiple drug metabolizing P450 enzymes. Results from $IC_{50}$ shift and TDI experiments, measuring the reversible and time dependent inhibition of several specific P450 metabolic activities in HLM, predict that the minor metabolite, DDEA, is responsible for precipitating drug interactions that arise as a consequence of inhibition of either CYP1A2 or CYP2C9 mediated metabolism, while both AMIO and MDEA appear to be important in DDIs resulting from inhibition of CYP2D6. Although DDEA is the strongest reversible inhibitor of CYP3A4 activity, MDEA shows a moderate ability to inactivate this enzyme. Thus, it is possible that both of these AMIO metabolites contribute to in vivo DDIs resulting from CYP3A4 inhibition. However, the observation that clinical DDIs (measured for the interactions of AMIO with lidocaine, warfarin, metoprolol and simvastatin) are in good agreement with predictions based solely on the reversible inhibition of CYP1A2, CYP2C9, CYP2D6 and CYP3A4 activities in HLM by parent

drug and metabolites would seem to suggest that TDI of these enzymes may not play a critical role in vivo.

**Authorship Contributions**

*Participated in research design:* McDonald, Au and Rettie

*Conducted experiments:* McDonald and Au

*Contributed new reagents or analytical tools:* McDonald

*Performed data analysis:* McDonald and Rettie

*Wrote or contributed to the writing of the manuscript:* McDonald and Rettie

## References

Becquemont L, Neuvonen M, Verstuyft C, Jaillon P, Letierce A, Neuvonen PJ and Funck-Brentano C (2007) Amiodarone interacts with simvastatin but not with pravastatin disposition kinetics. *Clin Pharmacol Ther* **81:**679-684.

Berry LM and Zhao Z (2008) An examination of IC50 and IC50-shift experiments in assessing time-dependent inhibition of CYP3A4, CYP2D6 and CYP2C9 in human liver microsomes. *Drug Metab Lett* **2:**51-59.

Castells DD, Teitelbaum BA and Tresley DJ (2002) Visual changes secondary to initiation of amiodarone: a case report and review involving ocular management in cardiac polypharmacy. *Optometry* **73:**113-121.

Chen Y, Mao J and Hop CE (2015) Physiologically based pharmacokinetic modeling to predict drug-drug interactions involving inhibitory metabolite: a case study of amiodarone. *Drug Metab Dispos* **43:**182-189.

Chitwood KK, Abdul-Haqq AJ and Heim-Duthoy KL (1993) Cyclosporine-amiodarone interaction. *Ann Pharmacother* **27:**569-571.

Dickstein G, Amikam S, Riss E and Barzilai D (1984) Thyrotoxicosis induced by amiodarone, a new efficient antiarrhythmic drug with high iodine content. *Am J Med Sci* **288:**14-17.

Doyle JF and Ho KM (2009) Benefits and risks of long-term amiodarone therapy for persistent atrial fibrillation: a meta-analysis. *Mayo Clin Proc* **84:**234-242.

Funck-Brentano C, Becquemont L, Kroemer HK, Buhl K, Knebel NG, Eichelbaum M and Jaillon P (1994) Variable disposition kinetics and electrocardiographic effects of flecainide during repeated dosing in humans: contribution of genetic factors, dose-dependent clearance, and interaction with amiodarone. *Clin Pharmacol Ther* **55:**256-269.

Ha HR, Bigler L, Wendt B, Maggiorini M and Follath F (2005) Identification and quantitation of novel metabolites of amiodarone in plasma of treated patients. *Eur J Pharm Sci* **24:**271-279.

Ha HR, Candinas R, Stieger B, Meyer UA and Follath F (1996) Interaction between amiodarone and lidocaine. *J Cardiovasc Pharmacol* **28:**533-539.

Hanson KL, VandenBrink BM, Babu KN, Allen KE, Nelson WL and Kunze KL (2010) Sequential metabolism of secondary alkyl amines to metabolic-intermediate complexes: opposing roles for the secondary hydroxylamine and primary amine metabolites of desipramine, (s)-fluoxetine, and N-desmethyldiltiazem. *Drug Metab Dispos* **38:**963-972.

Heger JJ, Prystowsky EN and Zipes DP (1983) Relationships between amiodarone dosage, drug concentrations, and adverse side effects. *Am Heart J* **106:**931-935.

Jefcoate CR (1978) Measurement of substrate and inhibitor binding to microsomal cytochrome P-450 by optical-difference spectroscopy. *Methods Enzymol* **52:**258-279.

Kobayashi K, Nakajima M, Chiba K, Yamamoto T, Tani M, Ishizaki T and Kuroiwa Y (1998) Inhibitory effects of antiarrhythmic drugs on phenacetin O-deethylation catalysed by human CYP1A2. *Br J Clin Pharmacol* **45:**361-368.

Liu Z and Franklin MR (1985) Cytochrome P-450 ligands: metyrapone revisited. *Arch Biochem Biophys* **241:**397-402.

Lucas AN, Tanol M, McIntosh MP and Rajewski RA (2006) Preparation and purification of desethylamiodarone hydrochloride. *Synthetic Communications* **36:**3371-3376.

Marchlinski FE, Gansler TS, Waxman HL and Josephson ME (1982) Amiodarone pulmonary toxicity. *Ann Intern Med* **97:**839-845.

Mason JW (1987) Amiodarone. *N Engl J Med* **316:**455-466.

McDonald MG, Au NT, Wittkowsky AK and Rettie AE (2012) Warfarin-amiodarone drug-drug interactions: determination of [I]u/Ki,u for amiodarone and its plasma metabolites. *Clin Pharmacol Ther* **91:**709-717.

Mori K, Hashimoto H, Takatsu H, Tsuda-Tsukimoto M and Kume T (2009) Cocktail-substrate assay system for mechanism-based inhibition of CYP2C9, CYP2D6, and CYP3A using human liver microsomes at an early stage of drug development. *Xenobiotica* **39:**415-422.

Nicolau DP, Uber WE, Crumbley AJ, 3rd and Strange C (1992) Amiodarone-cyclosporine interaction in a heart transplant patient. *J Heart Lung Transplant* **11:**564-568.

O'Reilly RA, Trager WF, Rettie AE and Goulart DA (1987) Interaction of amiodarone with racemic warfarin and its separated enantiomorphs in humans. *Clin Pharmacol Ther* **42:**290-294.

Obach RS, Walsky RL and Venkatakrishnan K (2007) Mechanism-based inactivation of human cytochrome p450 enzymes and the prediction of drug-drug interactions. *Drug Metab Dispos* **35:**246-255.

Ohyama K, Nakajima M, Suzuki M, Shimada N, Yamazaki H and Yokoi T (2000) Inhibitory effects of amiodarone and its N-deethylated metabolite on human cytochrome P450 activities: prediction of in vivo drug interactions. *Br J Clin Pharmacol* **49:**244-253.

Orlando R, Piccoli P, De Martin S, Padrini R, Floreani M and Palatini P (2004) Cytochrome P450 1A2 is a major determinant of lidocaine metabolism in vivo: effects of liver function. *Clin Pharmacol Ther* **75:**80-88.

Parkinson A, Kazmi F, Buckley DB, Yerino P, Paris BL, Holsapple J, Toren P, Otradovec SM and Ogilvie BW (2011) An evaluation of the dilution method for identifying metabolism-dependent inhibitors of cytochrome P450 enzymes. *Drug Metab Dispos* **39:**1370-1387.

Rigas B, Rosenfeld LE, Barwick KW, Enriquez R, Helzberg J, Batsford WP, Josephson ME and Riely CA (1986) Amiodarone hepatotoxicity. A clinicopathologic study of five patients. *Ann Intern Med* **104:**348-351.

Sadeque AJ, Eddy AC, Meier GP and Rettie AE (1992) Stereoselective sulfoxidation by human flavin-containing monooxygenase. Evidence for catalytic diversity between hepatic, renal, and fetal forms. *Drug Metab Dispos* **20:**832-839.

Sekiguchi N, Higashida A, Kato M, Nabuchi Y, Mitsui T, Takanashi K, Aso Y and Ishigai M (2009) Prediction of drug-drug interactions based on time-dependent inhibition from high throughput screening of cytochrome P450 3A4 inhibition. *Drug Metab Pharmacokinet* **24:**500-510.

Soto J, Sacristan JA, Arellano F and Hazas J (1990) Possible theophylline-amiodarone interaction. *DICP* **24:**1115.

Templeton IE, Thummel KE, Kharasch ED, Kunze KL, Hoffer C, Nelson WL and Isoherranen N (2008) Contribution of itraconazole metabolites to inhibition of CYP3A4 in vivo. *Clin Pharmacol Ther* **83:**77-85.

Thi L, Shaw D and Bird J (2009) Warfarin potentiation: a review of the "FAB-4" significant drug interactions. *Consult Pharm* **24:**227-230.

Trujillo TC and Nolan PE (2000) Antiarrhythmic agents - Drug interactions of clinical significance. *Drug Safety* **23:**509-532.

U.S. Food and Drug Administration (2006) Guidance for Industry Drug Interaction Studies - Study Design, Data Analysis, and Implications for Dosing and Labeling. Draft Guidance, Rockville, MD.

VandenBrink BM and Isoherranen N (2010) The role of metabolites in predicting drug-drug interactions: focus on irreversible cytochrome P450 inhibition. *Curr Opin Drug Discov Devel* **13:**66-77.

Varkhede NR, Jhajra S, Ahire DS and Singh S (2014) Metabolite identification studies on amiodarone in in vitro (rat liver microsomes, rat and human liver S9 fractions) and in vivo (rat feces, urine, plasma) matrices by using liquid chromatography with high-resolution mass spectrometry and multiple-stage mass spectrometry: Characterization of the diquinone metabolite supposedly responsible for the drug's hepatotoxicity. *Rapid Communications in Mass Spectrometry* **28:**311-331.

Waldhauser KM, Torok M, Ha HR, Thomet U, Konrad D, Brecht K, Follath F and Krahenbuhl S (2006) Hepatocellular toxicity and pharmacological effect of amiodarone and amiodarone derivatives. *J Pharmacol Exp Ther* **319:**1413-1423.

Wendt B, Ha HR and Hesse M (2002) Synthesis of two metabolites of the antiarrythmicum amiodarone. *Helvetica Chimica Acta* **85:**2990-3001.

Werner D, Wuttke H, Fromm MF, Schaefer S, Eschenhagen T, Brune K, Daniel WG and Werner U (2004) Effect of amiodarone on the plasma levels of metoprolol. *Am J Cardiol* **94:**1319-1321.

Yamreudeewong W, DeBisschop M, Martin LG and Lower DL (2003) Potentially significant drug interactions of class III antiarrhythmic drugs. *Drug Saf* **26:**421-438.

Yu H, Balani SK, Chen W, Cui D, He L, Humphreys WG, Mao J, Lai WG, Lee AJ, Lim HK, MacLauchlin C, Prakash C, Surapaneni S, Tse S, Upthagrove A, Walsky RL, Wen B and Zeng Z (2015) Contribution of metabolites to p450 inhibition-based drug-drug interactions: scholarship from the drug metabolism leadership group of the innovation and quality consortium metabolite group. *Drug Metab Dispos* **43:**620-630.

Yuan R, Madani S, Wei XX, Reynolds K and Huang SM (2002) Evaluation of cytochrome P450 probe substrates commonly used by the pharmaceutical industry to study in vitro drug interactions. *Drug Metab Dispos* **30:**1311-1319.

**Footnotes**

This work was supported by the National Institutes of Health grant [RO1–GM32165].

Please send reprint requests to: Allan E. Rettie, Department of Medicinal Chemistry, University of Washington, Box 37610, Seattle, WA, 98195, USA; tele: (206)685-0615; fax: (206)685-3252; email: rettie@u.washington.edu

**Figure Legends**

**Figure 1.** Amiodarone metabolites in human plasma.

**Figure 2.** Lineweaver-Burke plots showing inhibition of A) phenacetin O-dealkylation ($K_i$ = 723 ± 81 nM); B) diclofenac 4'-hydroxylation ($K_i$ = 308 ± 20 nM) and C) midazolam 1'-hydroxylation ($K_i$ = 1150 ± 380 nM) activities in pooled HLM by DDEA.

**Figure 3.** TDI experiments showing the inactivation profiles of A) phenacetin O-dealkylation activity in HLM by DDEA; B) dextromethorphan O-dealkylation activity in HLM by MDEA and C) midazolam 1'-hydroxylation activity in HLM by MDEA. Graph insets show plots of the slopes determined from the inactivation curves (λ) vs inhibitor concentration, with nonlinear regression fits to determine $K_I$ and $k_{inact}$ values. Slopes of the curves for the incubations containing no inhibitor were normalized to zero.

**Figure 4.** Type II P450 binding spectra are observed for DDEA bound to CYP1A2, CYP2C9 and CYP3A4. Experiments were performed with 200nM P450 Supersomes™ and 10 μM DDEA in 100mM KPi buffer, pH 7.4, at 25 °C.

**Figure 5.** Maximum MI complex spectra obtained from the incubations of DDEA with CYP1A2, and MDEA with CYP1A2, CYP2D6 and CYP3A4. Experiments

contained 10 μM inhibitor, 1 mM NADPH and either 110 nM P450 Supersomes™ (CYP2D6, CYP3A4) or 400 nM CYP1A2 Bactosomes™.

**Figure 6.** Comparison of AMIO N-dealkyase activity by A) a variety of recombinant P450 Supersomes™ and B) HLM with specific P450 chemical inhibition probes. Experiments were performed at 5 μM AMIO with either 20 pmol P450 Supersomes™ (A) or 1 mg/mL pooled HLM (B). Data represent the mean, with standard deviations, determined from triplicate incubations. aNF = α-naphthoflavone, FF = furafylline, MK = montelukast, SZ = sulfaphenazole, NBzN = N-benzylnirvanol, QD = quinidine, Ket = ketoconazole, TAO = troleandomycin.

**Figure 7.** Comparison of MDEA N-dealkyase activity by A) a variety of recombinant P450 Supersomes™ and B) HLM with specific P450 chemical inhibition probes. Experiments were performed at 5 μM MDEA with either 20 pmol P450 Supersomes™ (A) or 1 mg/mL pooled HLM (B). Data represent the mean, with standard deviations, determined from triplicate incubations. aNF = α-naphthoflavone, FF = furafylline, MK = montelukast, SZ = sulfaphenazole, NBzN = N-benzylnirvanol, QD = quinidine, Ket = ketoconazole, TAO = troleandomycin.

DMD Fast Forward. Published on August 21, 2015 as DOI: 10.1124/dmd.115.065623
This article has not been copyedited and formatted. The final version may differ from this version.



**Table 1. Reversible Inhibition of CYP1A2, CYP2C9, CYP2D6 and CYP3A4 Activities in HLM by AMIO and its Circulating Human Metabolites.**

| Inhibitor | CYP1A2[a] | | CYP2C9[b] | | CYP2D6[c] | | CYP3A4[d] | |
|---|---|---|---|---|---|---|---|---|
| | $IC_{50}$ (μM) | $[I]_u/K_{i,u}$ | $IC_{50}$ (μM) | $[I]_u/K_{i,u}$ | $IC_{50}$ (μM) | $[I]_u/K_{i,u}$ | $IC_{50}$ (μM) | $[I]_u/K_{i,u}$ |
| **AMIO** | >50 | <0.1 | >50 | <0.1 | 15 ± 9.5 | 0.34 | >50 | <0.1 |
| **MDEA** | >100 | <0.07 | 57 ± 9 | 0.07 | 17 ± 2.1 | 0.23 | 43 ± 5 | 0.09 |
| **DDEA** | 1.6 ± 0.42 | 0.28 | 0.64 ± 0.01 | 0.71 | 9.6 ± 2.8 | 0.05 | 1.8 ± 0.9 | 0.25 |
| **OH-MDEA** | >100 | <0.001 | 3.3 ± 1.4 | 0.03 | 5.3 ± 2.3 | 0.02 | 24 ± 0.7 | 0.01 |
| **ODAA** | >10 | <0.001 | 0.080 ± 0.034 | 0.08 | >10 | <0.001 | 8.6 ± 2.8 | 0.001 |
| **DAA** | >50 | <0.002 | >10 | <0.01 | >10 | <0.01 | >50 | <0.002 |

a. Phenacetin O-dealkylation was used as a probe for CYP1A2 activity in HLM

b. Diclofenac 4'-hydroxylation was used as a probe for CYP2C9 activity in HLM

c. Dextromethorphan O-dealkylation was used as a probe for CYP2D6 activity in HLM

d. Midazolam 1'-hydroxylation was used as a probe for CYP3A4 activity in HLM

$IC_{50}$ values are means, with standard error measurements, determined from (at least) duplicate experiments.

**Table 2. Comparison of predicted AMIO drug interactions vs observed clinical DDIs for drugs primarily metabolized by CYP1A2, CYP2C9, CYP2D6 or CYP3A4.**

| Pharmaceutical | In vivo DDI ($AUC_i/AUC$) | Predicted DDI: | | | |
|---|---|---|---|---|---|
| | | CYP1A2 | CYP2C9 | CYP2D6 | CYP3A4 |
| **Lidocaine** | 1.21 (Ha et al., 1996) | 1.28 | | | |
| **S-Warfarin** | 2.10 (O'Reilly et al., 1987) | | 1.89 | | |
| **Metoprolol** | 1.94 (Werner et al., 2004) | | | 1.64 | |
| **Simvastatin** | 1.76 (Becquemont et al., 2007) | | | | 1.35 |
| **R-Warfarin** | 1.62 (O'Reilly et al., 1987) | | | | 1.35 |

Predicted interactions are based on the sum of $[I]_u/K_{i,u}$ data (Equation 1) determined for the reversible inhibition of specific P450 substrate probes by AMIO and its circulating human metabolites (Table 1).

DMD Fast Forward. Published on August 21, 2015 as DOI: 10.1124/dmd.115.065623
This article has not been copyedited and formatted. The final version may differ from this version.

DMD Fast Forward. Published on August 21, 2015 as DOI: 10.1124/dmd.115.065623
This article has not been copyedited and formatted. The final version may differ from this version.

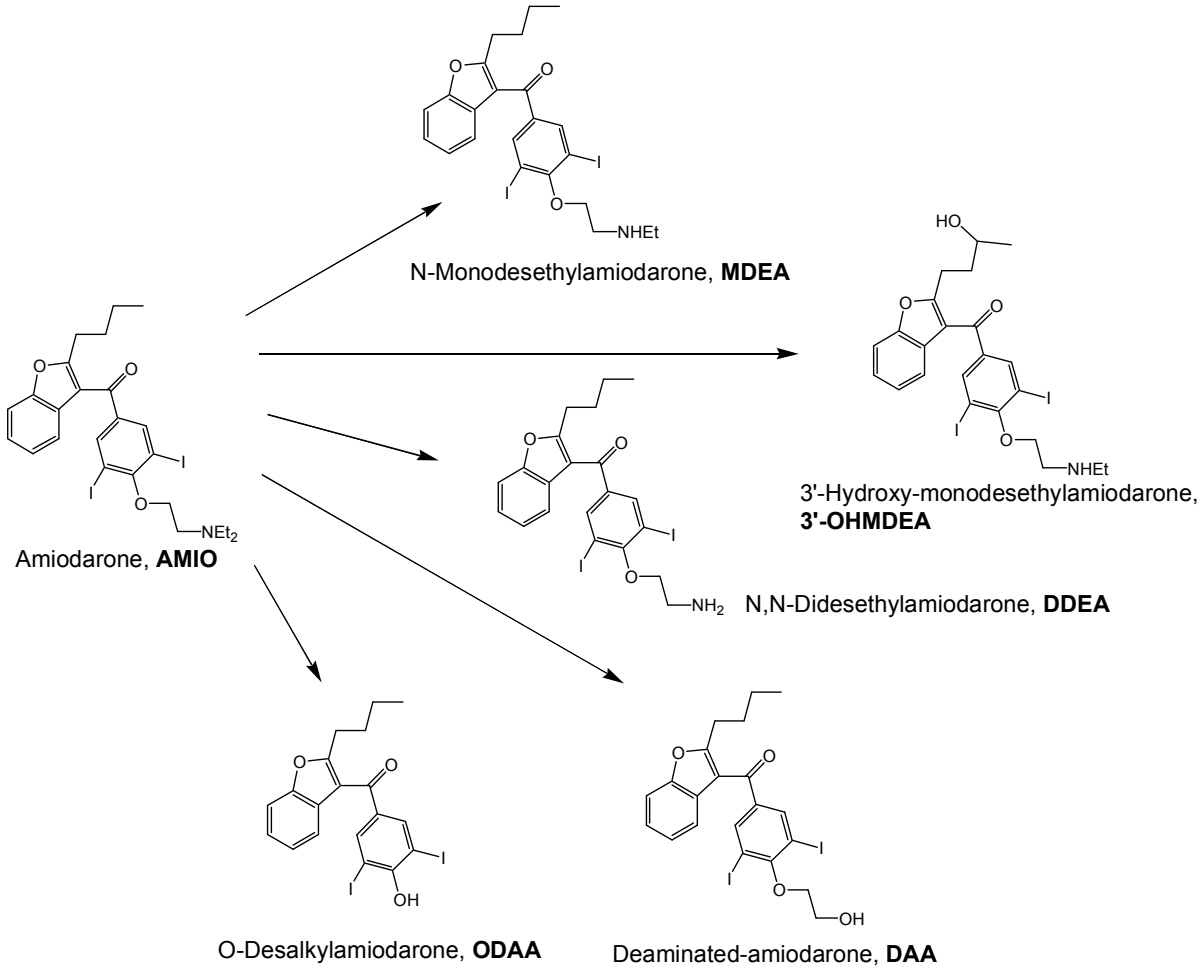


**Figure 1**

DMD Fast Forward. Published on August 21, 2015 as DOI: 10.1124/dmd.115.065623
This article has not been copyedited and formatted. The final version may differ from this version.

**A**

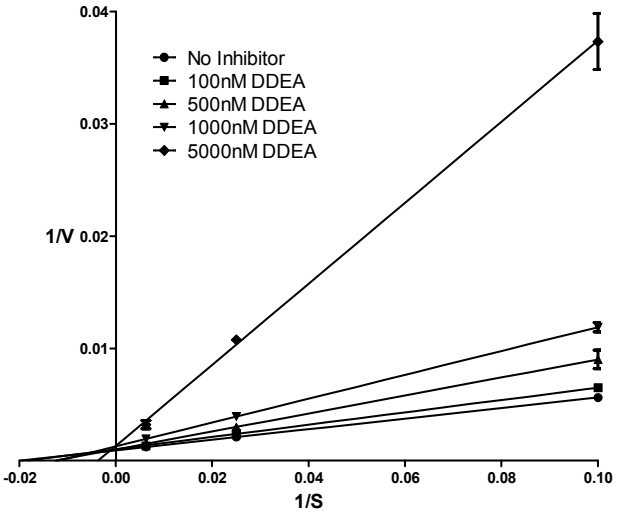


**B**

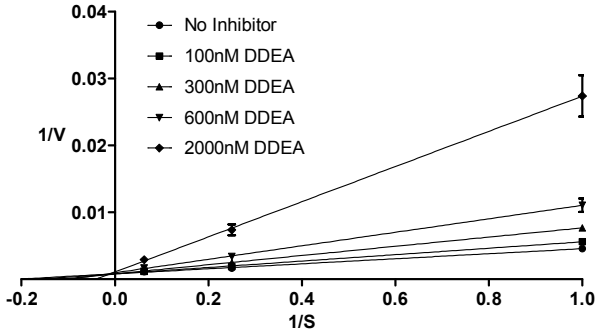


**C**

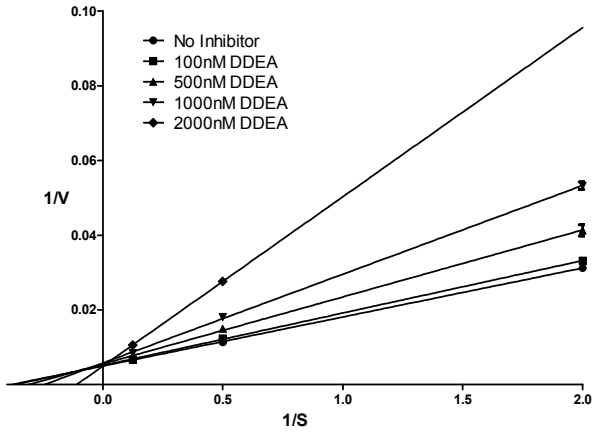


**Figure 2**

DMD Fast Forward. Published on August 21, 2015 as DOI: 10.1124/dmd.115.065623
This article has not been copyedited and formatted. The final version may differ from this version.

**A**

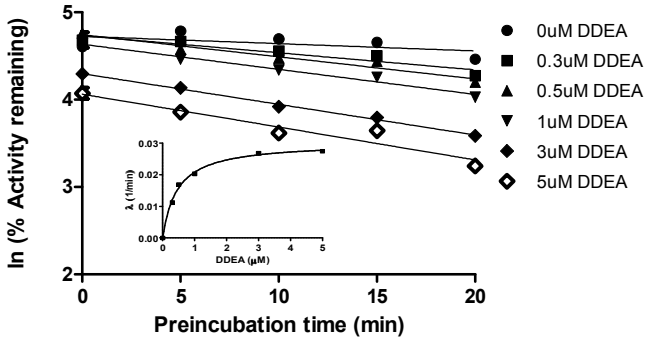


**B**

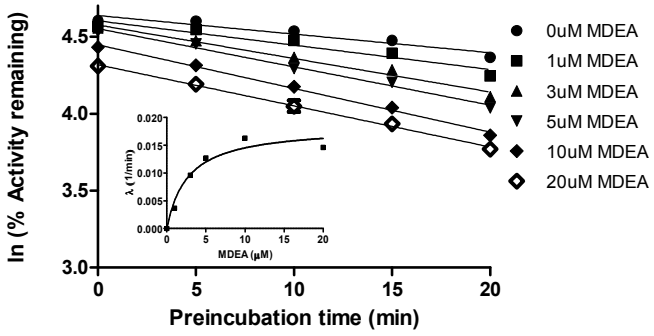


**C**

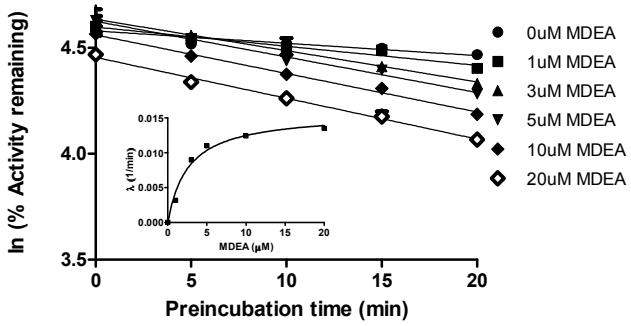


**Figure 3**

DMD Fast Forward. Published on August 21, 2015 as DOI: 10.1124/dmd.115.065623
This article has not been copyedited and formatted. The final version may differ from this version.

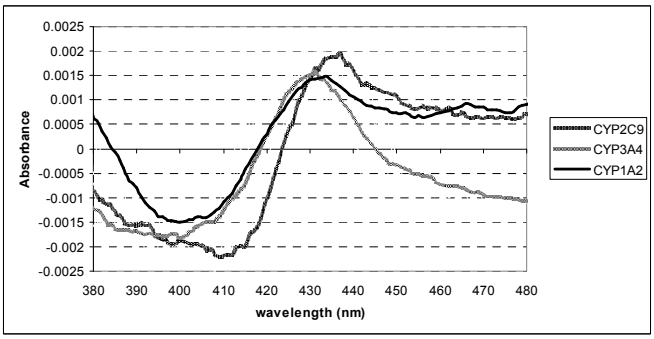


**Figure 4**

DMD Fast Forward. Published on August 21, 2015 as DOI: 10.1124/dmd.115.065623
This article has not been copyedited and formatted. The final version may differ from this version.

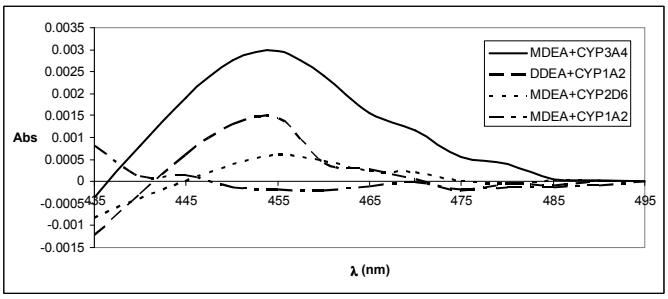


**Figure 5**

DMD Fast Forward. Published on August 21, 2015 as DOI: 10.1124/dmd.115.065623
This article has not been copyedited and formatted. The final version may differ from this version.

**A**

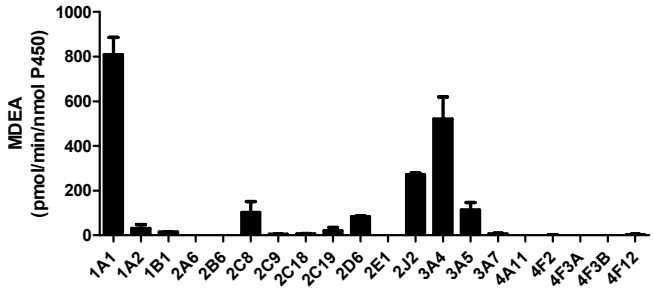


**B**

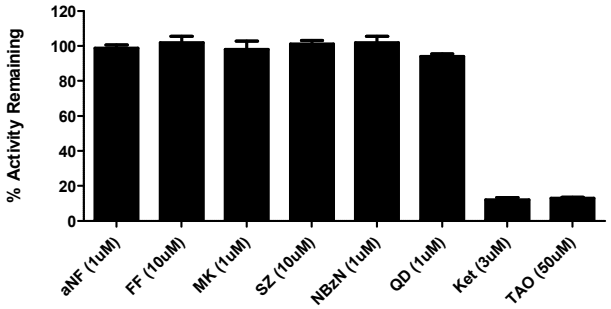


**Figure 6**

DMD Fast Forward. Published on August 21, 2015 as DOI: 10.1124/dmd.115.065623
This article has not been copyedited and formatted. The final version may differ from this version.

**A.**

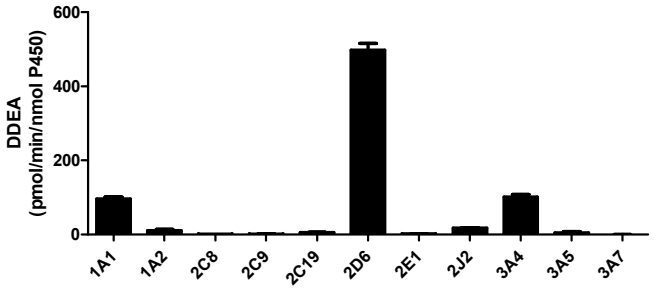


**B**

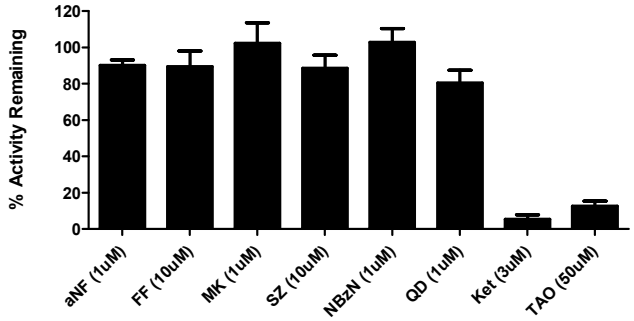


**Figure 7**